SARS-CoV-2 spike protein binds heparan sulfate in a length- and sequence-dependent manner

Lin Liu,[1,5] Pradeep Chopra,[1,5] Xiuru Li,[1,5] Margreet A. Wolfert,[1,3] S. Mark Tompkins,[2] and Geert-Jan Boons[1,3,4,*]

[1]Complex Carbohydrate Research Center, University of Georgia, 315 Riverbend Road, Athens, GA 30602, USA

[2]Center for Vaccines and Immunology, University of Georgia, Athens, GA 30602, USA

[3]Department of Chemical Biology and Drug Discovery, Utrecht Institute for Pharmaceutical Sciences, and Bijvoet Center for Biomolecular Research, Utrecht University, Universiteitsweg 99, 3584 CG Utrecht, The Netherlands

[4]Department of Chemistry, University of Georgia, Athens, GA 30602, USA

[5]These authors contributed equally to this work

*Corresponding author. E-mail: G.J.H.P.Boons@uu.nl or gjboons@ccrc.uga.edu

ABSTRACT

Severe acute respiratory syndrome-related coronavirus 2 (SARS-CoV-2) is causing an unprecedented global pandemic demanding the urgent development of therapeutic strategies. Microarray binding experiments using an extensive heparan sulfate (HS) oligosaccharide library showed the spike of SARS-CoV-2 can bind HS in a length- and sequence-dependent manner. Hexa- and octasaccharides composed of IdoA2S-GlcNS6S repeating units were identified as optimal ligands. Surface plasma resonance (SPR) showed the SARS-CoV-2 spike protein binds with higher affinity to heparin (K_D 55 nM) compared to the receptor binding domain (RBD, K_D 1 μM) alone. An octasaccharide composed of IdoA2S-GlcNS6S could inhibit spike-heparin interaction with an IC_{50} of 38 nM. Our data supports a model in which the RBD of the spike of SARS-CoV-2 confers sequence specificity for HS expressed by target cells whereas an additional HS binding site in the S1/S2 proteolytic cleavage site enhances the avidity of binding. Collectively, our results highlight the potential of using HS oligosaccharides as a therapeutic agent by inhibiting SARS-CoV-2 binding to target cells.

KEYWORDS

SARS-CoV-2, coronavirus, heparan sulfate, heparin, spike glycoprotein, microarray, surface plasma resonances

INTRODUCTION

The SARS-CoV-2 pandemic demands the urgent development of therapeutic strategies. An attractive approach is to interfere in the attachment of the virus to the host cell. The entry of SARS-CoV-2 into cells is initiated by binding of the transmembrane spike (S) glycoprotein of the virus to angiotensin-converting enzyme 2 (ACE2) of the host.[1] SARS-CoV is closely related to SARS-CoV-2 and employs the same receptor.[2] The spike protein of SARS-CoV-2 is comprised of two subunits; S1 is responsible for binding to the host receptor, whereas S2 promotes membrane fusion. The C terminal domain (CTD) of S1 harbors the receptor binding domain (RBD).[3]

It is known that the spike protein of number of human coronaviruses can bind to a secondary receptor, or co-receptor, to facilitate cell entry. For example, MERS-CoV employs sialic acid as co-receptor along its main receptor DPP4.[4] Human CoV-NL63, which also utilizes ACE2 as receptor, uses heparan sulfate (HS) proteoglycans, as co-receptor.[5] It has also been shown that entry of SARS-CoV pseudo-typed virus into Vero E6 and Caco-2 cells can significantly be inhibited by heparin or treatment with heparinase, indicating the importance of HS for infectivity.[6]

There are indications that the SARS-CoV-2 spike also interacts with HS. One reports showed that heparin can induce a conformation change in the RBD of SARS-CoV-2.[7] A combined SPR and computational study showed that glycosaminoglycans can bind to the proteolytic cleavage site of the S1 and S2 protein.[8]

HS are highly complex *O*- and *N*- sulfated polysaccharides that reside as major components on the cell surface and extracellular matrix of all eukaryotic cells.[9] Various proteins interact with HS thereby regulating many biological and disease processes, including cell adhesion, proliferation, differentiation and inflammation. They are also used by many viruses, including herpes simplex virus (HSV), Dengue virus, HIV, and various coronaviruses, as receptor or co-receptor.[10-12]

The biosynthesis of HS is highly regulated and the length and degree and pattern of sulfation of HS can differ substantially between different cell types. The so-called "*HS sulfate code hypothesis"* is based on the notion that expression of specific HS epitopes by cells makes it possible to recruit specific HS-binding proteins, thereby controlling a multitude of biological processes.[13-14] In support of this hypothesis, several studies have

shown that HS binding proteins exhibit preferences for specific HS oligosaccharide motifs.[15-16] Therefore, we were compelled to investigate whether the spike of SARS-CoV-2 recognizes specific HS motifs. Such insight is expected to pave the way to develop inhibitors of viral cell binding and entry.

Previously, we prepared an unprecedented library of structurally well-defined heparan sulfate oligosaccharides that differ in chain length, backbone composition an sulfation pattern.[17-18] This collection of HS oligosaccharides was used to develop a glycan microarray for the systematic analysis of binding selectivities of HS-binding proteins. Using this microarray platform in conjugation with detailed binding studies, we found that the SARS-CoV-2-S can bind HS in a length- and sequence-dependent manner. We propose a model for HS mediated cell binding and entry.

RESULTS AND DISCUSSION

A HS microarray was fabricated having well over 100 unique di-, tetra- hexa- and octasaccharides differing in backbone composition and sulfation pattern (**Fig. 1C**). The synthetic HS oligosaccharides contain an aminopentyl spacer allowing printing on *N*-hydroxysuccinimide (NHS)-active glass slides for microarray fabrication. All oligosaccharides were printed at 100 μM concentration in replicates of 6 by non-contact piezoelectric printing. The quality of the HS microarray was validated using various well characterized HS-binding proteins.

The spike glycoprotein of SARS-CoV-2 (S1+S2, extra cellular domain, amino acid residue 1-1213) was expressed in insect cells having a C-terminal His-tag.[19] Recombinant SARS-CoV-2-RBD, containing amino acid residue 319-541, was expressed in HEK293 cells also with a C-terminal His-tag.[19]

Sub-arrays were incubated with different concentrations of the proteins in a binding buffer (pH 7.4, 20 mM Tris, 150 mM NaCl, 2 mM $CaCl_2$, 2 mM $MgCl_2$ with 1% BSA and 0.05% Tween-20) at room temperature for 1 h. After washing and drying, the subarrays were exposed to an anti-His antibody labeled with AlexaFluor® 647 for another hour. Binding was established by fluorescent scanning and the resulting data was processed using home-written software.

To analyze the data, the compounds were arranged according to increasing backbone length, and within each group with increasing numbers of sulfates. Intriguingly, the proteins showed a strong preference for specific HS oligosaccharides (**Fig. 1A**, **B**). Furthermore, it was found that SARS-CoV-2-spike and the RBD have similar selectivities. Compounds showing strong responsiveness (**77**, **78**, **79**, and **81**) are composed of tri-sulfated repeating units (IdoA2S-GlcNS6S). The binding is length-dependent and HS oligosaccharide **81** $(IdoA2S\text{-}GlcNS6S)_4$ and **79** $(IdoA2S\text{-}GlcNS6S)_3$ having four and three repeating units, respectively, showed the strongest binding. On the other hand, tetrasaccharide **57** $(IdoA2S\text{-}GlcNS6S)_2$, which has the same repeating unit structure, gave a very low responsiveness. A similar observation was made for disaccharide **4** (IdoA2S-GlcNS6S).

The structure-binding data shows that perturbations in the backbone or sulfation pattern lead to substantial reductions in binding. The importance of the IdoA2S residue is highlighted by comparing hexasaccharides **79** with **77** in which a single IdoA2S in the distal disaccharide repeating unit is replaced with GlcA. This modification lead to a substantial reduction in responsiveness. Further replacements of IdoA2S with GlcA in compound **77** completely abolish binding, as evident for compounds **70**, **68**, and **62**. The structure-activity data also showed that the 2-*O*-sulfates are crucial, and binding was lost when such functionalities were not present (**77** *vs.* **71**, **69**, and **65**). Lack of one or more 6-*O*-sulfates also resulted in substantial reductions in binding (**77** *vs.* **72** and **66**). Although the SARS-CoV-2 spike and RBD showed similar selectivities, the binding of the spike appeared stronger and much higher fluorescent readings were observed at the same protein concentration.

To validate the microarray results, binding experiments were performed by surface plasma resonances (SPR). Biotinylated heparin was immobilized on a streptavidin-coated sensor chip and binding experiments were performed with different concentrations of the spike protein and RBD. Representative sensorgrams are shown in **Fig. 2**. K_D values of 55 nM and 1.0 μM were determined using a 1:1 Langmuir binding model for the spike and RBD, respectively. A previous reported computational study indicated that in addition to the RBD, another HS-binding site may reside in the S1/S2 proteolytic cleavage site of the

spike.[8] Our data support a model in which the HS binding site of the RBD confers sequence specificity whereas that in S1/S2 proteolytic cleavage site enhances the affinity.

Next, we examined whether HS oligosaccharide **81** can interfere in the interaction of the spike or RBD with immobilized heparin. Thus, the spike protein (150 nM) or RBD (2.4 μM) were pre-mixed with different concentrations of compound **81** and then used as analytes. The IC_{50} values were determined by non-linear fitting of Log(inhibitor) *vs.* response using variable slope (**Fig. 3**). The IC_{50} values for the spike protein and RBD are 38 nM and 264 nM, respectively, showing compound **81** is a potent competitive inhibitor of the interaction of SARS-CoV-2 spike with heparin.

DISCUSSION AND CONCLUSIONS

The microarray and SPR results presented here demonstrate that the spike of SARS-CoV-2 can bind HS in a length- and sequence-dependent manner. Hexa- and octasaccharides composed of IdoA2S-GlcNS6S repeating units have been defined as optimal ligands. Our data supports a model in which the RBD of the spike confers sequence specificity and an additional HS binding site in the S1/S2 proteolytic cleavage site[8] enhances the avidity of binding probably by non-specific interactions.

Although the IdoA2S-GlcNS6S is abundantly present in heparin, it is a minor component of HS.[20] Interestingly, it has been reported that the expression of the $(GlcNS6S\text{-}IdoA2S)_3$ motif is highly regulated and plays a crucial role in cell behavior and disease including endothelial cell activation.[21] Severe thrombosis in COVID-19 patients is associated with endothelial dysfunction[22] and a connection may exist between SARS-CoV-2's ability to bind to HS and thrombotic disorder.

The current clinical guidelines calls for the use of unfractionated heparin or low molecular weight heparin (LMWH) for the treatment of *all* COVID-19 patients for systemic clotting in the absences of contradictions.[23-24] Our findings indicate that heparin treatment may have additional benefits, and may compete with the binding of the spike protein to cell surface HS thereby preventing infectivity. It suggests that *non-coagulating* heparin or HS preparations can be developed that reduce cell binding and infectivity without a risk of causing bleeding. In this respect, administration of heparin requires great care because its anticoagulant activity can result in excessive bleeding. Antithrombin III

(ATIII), which confers anticoagulant activity, binds a specific pentasaccharide GlcNAc(6S)-GlcA-GlcNS(3S)(6S)-IdoA2S-GlcNS(6S) embedded in HS or heparin. Removal of the sulfate at C-3 of *N*-sulfoglucosamine (GlcNS3S) of the pentasaccharide results in a 10^5-fold reduction in binding affinity.[25] Importantly, such a functionality is not present in the identified HS ligand of SARS-CoV-2 spike, and therefore compounds can be developed that can inhibit cell binding, but do not interact with ATIII. As a result, such preparations can be used at higher doses without causing adverse side effects. Our data also shows that multivalent interactions of the spike with HS results in high avidity of binding. This observation provides opportunities to develop glycopolymers modified by HS oligosaccharides as to inhibitors of SARS-CoV-2 cell binding to prevent or treat COVID-19.

EXPERIMENTAL SECTION

Materials

The SARS-CoV-2-spike (S1+S2) was obtained from Sino Biological (40589-V08B1). The Alexa Fluor 647 anti-His tag antibody was obtained from BioLegend (#652513). The Heparin Amine (heparin functionalized with primary amine, Mw 27k) on microarray was obtained from Creative PEGWorks (HP-230). High grade heparin (HG-Hep, Mw 15,700) for SPR was obtained from Iduron Ltd, UK (#HEP-HG 100).

Expression of SARS-CoV-2-RBD

The RBD modified by an His6-tag was expressed in HEK cell as previously described.[19]

Microarray printing and screening

All compounds were printed on NHS-ester activated glass slides (NEXTERION® Slide H, Schott Inc.) using a Scienion sciFLEXARRAYER S3 non-contact microarray equipped with a Scienion PDC80 nozzle (Scienion Inc.). Individual samples were dissolved in sodium phosphate buffer (50 µL, 0.225 M, pH 8.5) at a concentration of 100 µM and were printed in replicates of 10 with spot volume ~ 400 pL, at 20 °C and 50% humidity. Each slide has 24 subarrays in a 3x8 layout. After printing, slides were incubated in a humidity

chamber for 8 h and then blocked for 30 min with a 5mM ethanolamine in a Tris buffer (pH 9.0, 50 mM) at 40 °C. Blocked slides were rinsed with DI water, spun dry, and kept in a desiccator at room temperature for future use.

Screening was performed by incubating the slides with a protein solution for a certain amount of time followed by washing and drying. A typical washing procedure includes sequentially dipping the glass slide in TSM wash buffer (2 min, containing 0.05 % Tween 20), TSM buffer (2 min) and, water (2 x 2 min), followed by spun dry. For SARS-CoV-2-RBD and SARS-CoV-2-Spike protein screening, the slides were incubated with SARS-CoV-2-RBD (10, 30, and 100 µg/mL in TSMBB) or SARS-CoV-2-Spike (3, 10, and 30 µg/mL in TSMBB) for 1 h, followed by washing and incubated with a solution of AlexaFluor® 647 conjugated anti-His antibody (10 µg/mL). After washing and drying, the slides were scanned using a GenePix 4000B microarray scanner (Molecular Devices) at the appropriate excitation wavelength with a resolution of 5 µM. Various gains and PMT values were employed for the scanning to ensure that all the signals were within the linear range of the scanner's detector and there was no saturation of signals. The images were analyzed using GenePix Pro 7 software (version 7.2.29.2, Molecular Devices). The data was analyzed with our home written Excel macro to provide the results. The highest and the lowest value of the total fluorescence intensity of the replicates spots were removed, and the remaining values were used to provide the mean value and standard deviation.

Preparation of biotinylated heparin

High grade heparin (HG-Hep, Mw 15,700, Iduron, UK) was biotinylated following a literature procedure.[26] Briefly, HG-Hep (0.5 mg), biotin-$(PEG)_3$-NH_2 (0.5 mg, Thermo Scientific, USA) and sodium cyanoborohydride (2.5 mg, $NaBH_3CN$, AminoLink™ reductant, Thermo Scientific, USA) were combined, dissolved in water (100 µL) and stirred at 70 °C for 24 h. Another portion of $NaBH_3CN$ (2.5 mg) was added and stirring continued for additional 24 h. To remove excess of biotin linker and reductant, the reaction mixture was filter centrifuged (Mw cutoff 3000) and exchanged with water (2x1 mL, Milli-Q®), concentrated (200 µL) and lyophilized to obtain the desired Biotin-HG-Hep as white fluffy powder. The product was aliquoted and stored at -80 °C.

Surface plasma resonances experiments

A streptavidin coated chip was prepared from a CM5 chip by standard amine coupling using an amine coupling kit (Biacore Inc. - GE Healthcare). Briefly, the surface was activated using freshly mixed *N*-hydroxysuccinimide (NHS; 100 mM) and 1-(3-dimethylaminopropyl)-ethylcarbodiimide (EDC; 391 mM) (1/1, v/v) in water. The remaining active esters were quenched by aqueous ethanolamine (1.0 M; pH 8.5). Next, streptavidin (50 µg/mL) in aqueous NaOAc (10 mM, pH 4.5) was passed over the chip surface until a ligand density of approximately 3,000 RU was achieved. Next, biotin-HG-Hep (1 µM) was passed over one of the flow channels at a flow rate of 5 µL/min for two min resulting in a response of 56 RU. Next, the reference and modified flow cells were washed with three consecutive injections of 1 min with 1 M NaCl in 50 mM NaOH. HBS-EP (0.01 M HEPES, 150 mM NaCl, 3 mM EDTA, 0.005% polysorbate 20; pH 7.4) was used as the running buffer for the immobilization, kinetic studies of the interaction of HG-Hep with SARS-CoV-2-RBD and spike protein (S1+S2), and inhibition studies of immobilized HG-Hep with synthetic GAGs oligosaccharides. Analytes were dissolved in running buffer and a flow rate of 30µL/min was employed for association and dissociation at a constant temperature of 25 ^{o}C. A 60 s injection of 0.25% sodium dodecyl sulfonate (SDS) at a flow rate of 30 µl/min was used for regeneration and to achieve prior baseline status. Using Biacore T100 evaluation software, the response curves of various analyte concentrations were globally fitted to the 1:1 binding model.

ACKNOWLEDGMENTS

This research was supported by the National Institute of General Medicine (NIGMS; Research Resource for Integrated Glycotechnology P41GM103390 to G.-J.B.).

REFERENCES

1. Walls, A. C.; Park, Y.-J.; Tortorici, M. A.; Wall, A.; McGuire, A. T.; Veesler, D., Structure, Function, and Antigenicity of the SARS-CoV-2 Spike Glycoprotein. *Cell* **2020,** *181* (2), 281-292.e6.
2. Li, F.; Li, W.; Farzan, M.; Harrison, S. C., Structure of SARS Coronavirus Spike Receptor-Binding Domain Complexed with Receptor. *Science* **2005,** *309* (5742), 1864-1868.
3. Monteil, V.; Kwon, H.; Prado, P.; Hagelkrüys, A.; Wimmer, R. A.; Stahl, M.; Leopoldi, A.; Garreta, E.; Hurtado del Pozo, C.; Prosper, F.; Romero, J. P.; Wirnsberger, G.; Zhang, H.; Slutsky, A. S.; Conder, R.; Montserrat, N.; Mirazimi, A.; Penninger, J. M., Inhibition of SARS-CoV-2 Infections in Engineered Human Tissues Using Clinical-Grade Soluble Human ACE2. *Cell* **2020,** *181* (1), 1-9.
4. Li, W.; Hulswit, R. J. G.; Widjaja, I.; Raj, V. S.; McBride, R.; Peng, W.; Widagdo, W.; Tortorici, M. A.; van Dieren, B.; Lang, Y.; van Lent, J. W. M.; Paulson, J. C.; de Haan, C. A. M.; de Groot, R. J.; van Kuppeveld, F. J. M.; Haagmans, B. L.; Bosch, B.-J., Identification of sialic acid-binding function for the Middle East respiratory syndrome coronavirus spike glycoprotein. *Proc. Natl. Acad. Sci.* **2017,** *114* (40), E8508-E8517.
5. Milewska, A.; Zarebski, M.; Nowak, P.; Stozek, K.; Potempa, J.; Pyrc, K., Human Coronavirus NL63 Utilizes Heparan Sulfate Proteoglycans for Attachment to Target Cells. *J. Virol.* **2014,** *88* (22), 13221-13230.
6. Lang, J.; Yang, N.; Deng, J.; Liu, K.; Yang, P.; Zhang, G.; Jiang, C., Inhibition of SARS Pseudovirus Cell Entry by Lactoferrin Binding to Heparan Sulfate Proteoglycans. *PLoS One* **2011,** *6* (8), e23710.
7. Mycroft-West, C.; Su, D.; Elli, S.; Li, Y.; Guimond, S.; Miller, G.; Turnbull, J.; Yates, E.; Guerrini, M.; Fernig, D.; Lima, M.; Skidmore, M., The 2019 coronavirus (SARS-CoV-2) surface protein (Spike) S1 Receptor Binding Domain undergoes conformational change upon heparin binding. *bioRxiv* **2020**, 2020.02.29.971093.
8. Kim, S. Y.; Jin, W.; Sood, A.; Montgomery, D. W.; Grant, O. C.; Fuster, M. M.; Fu, L.; Dordick, J. S.; Woods, R. J.; Zhang, F.; Linhardt, R. J., Glycosaminoglycan binding motif at S1/S2 proteolytic cleavage site on spike glycoprotein may facilitate novel coronavirus (SARS-CoV-2) host cell entry. *bioRxiv* **2020**, 2020.04.14.041459.
9. Bishop, J. R.; Schuksz, M.; Esko, J. D., Heparan sulphate proteoglycans fine-tune mammalian physiology. *Nature* **2007,** *446* (7139), 1030-1037.
10. Cagno, V.; Tseligka, E. D.; Jones, S. T.; Tapparel, C., Heparan Sulfate Proteoglycans and Viral Attachment: True Receptors or Adaptation Bias? *Viruses* **2019,** *11* (7), 596.
11. de Haan, C. A. M.; Haijema, B. J.; Schellen, P.; Wichgers Schreur, P.; te Lintelo, E.; Vennema, H.; Rottier, P. J. M., Cleavage of group 1 coronavirus spike proteins: how furin cleavage is traded off against heparan sulfate binding upon cell culture adaptation. *J. Virol.* **2008,** *82* (12), 6078-6083.
12. de Haan, C. A. M.; Li, Z.; te Lintelo, E.; Bosch, B. J.; Haijema, B. J.; Rottier, P. J. M., Murine coronavirus with an extended host range uses heparan sulfate as an entry receptor. *J. Virol.* **2005,** *79* (22), 14451-14456.
13. Sarrazin, S.; Lamanna, W. C.; Esko, J. D., Heparan sulfate proteoglycans. *Cold Spring Harb. Perspect. Biol.* **2011,** *3* (7), a004952.

14. Xu, D.; Esko, J. D., Demystifying Heparan Sulfate–Protein Interactions. *Annu. Rev. Biochem* **2014,** *83* (1), 129-157.
15. Kamhi, E.; Joo, E. J.; Dordick, J. S.; Linhardt, R. J., Glycosaminoglycans in infectious disease. *Biological Reviews* **2013,** *88* (4), 928-943.
16. García, B.; Merayo-Lloves, J.; Martin, C.; Alcalde, I.; Quirós, L. M.; Vazquez, F., Surface Proteoglycans as Mediators in Bacterial Pathogens Infections. *Front. Microbiol.* **2016,** *7*, 220.
17. Zong, C.; Venot, A.; Li, X.; Lu, W.; Xiao, W.; Wilkes, J.-S. L.; Salanga, C. L.; Handel, T. M.; Wang, L.; Wolfert, M. A.; Boons, G.-J., Heparan Sulfate Microarray Reveals That Heparan Sulfate–Protein Binding Exhibits Different Ligand Requirements. *J. Am. Chem. Soc.* **2017,** *139* (28), 9534-9543.
18. Arungundram, S.; Al-Mafraji, K.; Asong, J.; Leach, F. E.; Amster, I. J.; Venot, A.; Turnbull, J. E.; Boons, G.-J., Modular Synthesis of Heparan Sulfate Oligosaccharides for Structure−Activity Relationship Studies. *J. Am. Chem. Soc.* **2009,** *131* (47), 17394-17405.
19. Wu, F.; Zhao, S.; Yu, B.; Chen, Y.-M.; Wang, W.; Song, Z.-G.; Hu, Y.; Tao, Z.-W.; Tian, J.-H.; Pei, Y.-Y.; Yuan, M.-L.; Zhang, Y.-L.; Dai, F.-H.; Liu, Y.; Wang, Q.-M.; Zheng, J.-J.; Xu, L.; Holmes, E. C.; Zhang, Y.-Z., A new coronavirus associated with human respiratory disease in China. *Nature* **2020,** *579* (7798), 265-269.
20. Rabenstein, D. L., Heparin and heparan sulfate: structure and function. *Nat. Prod. Rep.* **2002,** *19* (3), 312-331.
21. Smits, N. C.; Kurup, S.; Rops, A. L.; ten Dam, G. B.; Massuger, L. F.; Hafmans, T.; Turnbull, J. E.; Spillmann, D.; Li, J.-p.; Kennel, S. J.; Wall, J. S.; Shworak, N. W.; Dekhuijzen, P. N. R.; van der Vlag, J.; van Kuppevelt, T. H., The Heparan Sulfate Motif (GlcNS6S-IdoA2S)3, Common in Heparin, Has a Strict Topography and Is Involved in Cell Behavior and Disease. *J. Biol. Chem.* **2010,** *285* (52), 41143-41151.
22. Sardu, C. G., J.; Morelli, M.B.; Wang, X.; Marfella, R.; Santulli, G. , Is COVID-19 an Endothelial Disease? Clinical and Basic Evidence. . *Preprints* **2020**, 2020040204.
23. Tang, N.; Bai, H.; Chen, X.; Gong, J.; Li, D.; Sun, Z., Anticoagulant treatment is associated with decreased mortality in severe coronavirus disease 2019 patients with coagulopathy. *J. Thromb. Haemost.* **2020,** *18* (5), 1094-1099.
24. Thachil, J.; Tang, N.; Gando, S.; Falanga, A.; Cattaneo, M.; Levi, M.; Clark, C.; Iba, T., ISTH interim guidance on recognition and management of coagulopathy in COVID-19. *J. Thromb. Haemost.* **2020,** *18* (5), 1023-1026.
25. Thacker, B. E.; Xu, D.; Lawrence, R.; Esko, J. D., Heparan sulfate 3-O-sulfation: a rare modification in search of a function. *Matrix Biol.* **2014,** *35*, 60-72.
26. Zhang, F.; Zheng, L.; Cheng, S.; Peng, Y.; Fu, L.; Zhang, X.; Linhardt, R. J., Comparison of the Interactions of Different Growth Factors and Glycosaminoglycans. *Molecules* **2019,** *24* (18), 3360.

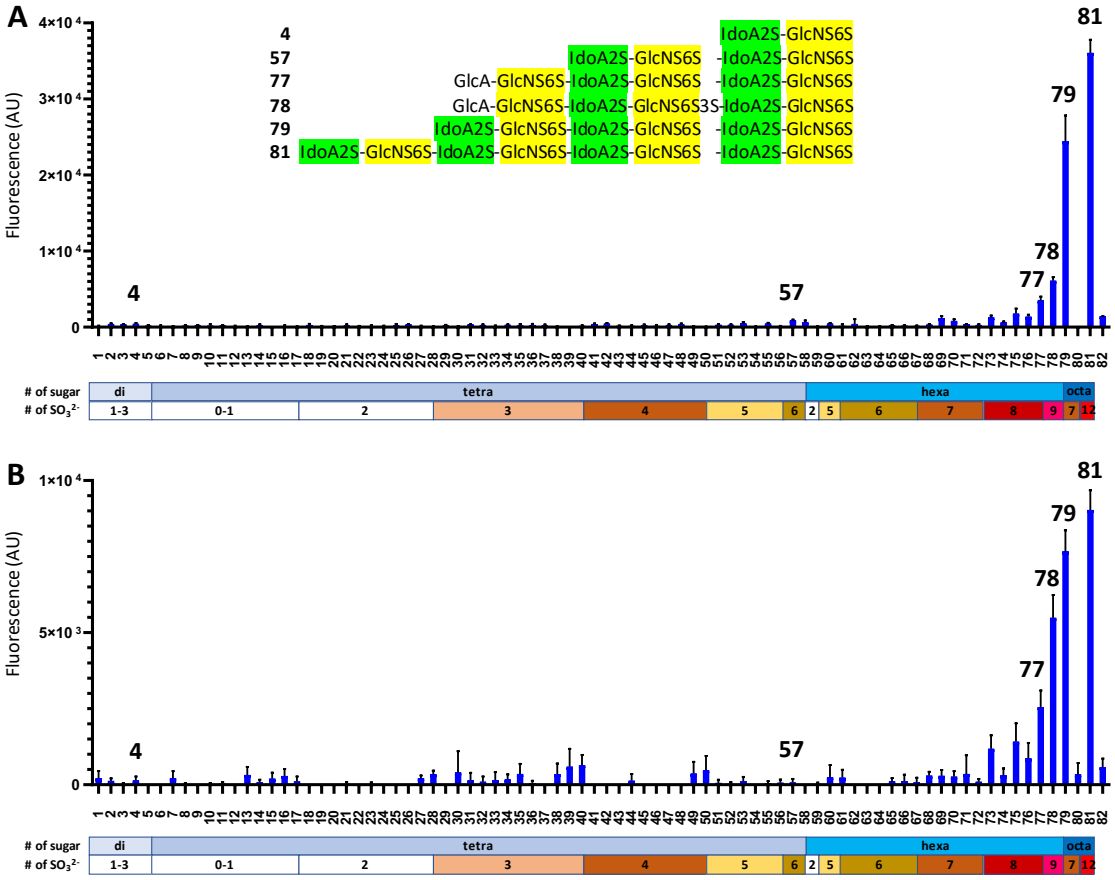

C

1	IdoA-GlcNAc6S	**29**	GlcA-GlcNAc6S-IdoA2S-GlcNAc6S	**56**	GlcA-GlcNS6S-GlcA2S-GlcNS6S
2	GlcA-GlcNAc6S	**30**	IdoA-GlcNAc6S-IdoA2S-GlcNAc6S	**57**	IdoA2S-GlcNS6S-IdoA2S-GlcNS6S
3	IdoA2S-GlcNAc6S	**31**	GlcA-GlcNS-IdoA2S-GlcNS	**58**	GlcA-GlcNS3S6S-IdoA2S-GlcNS6S
4	IdoA2S-GlcNS6S	**32**	GlcA-GlcNS-GlcA2S-GlcNS	**59**	GlcA-GlcNAc-IdoA2S-GlcNAc6S-GlcA-GlcNAc
5	IdoA2S-GlcNS6S	**33**	GlcA-GlcNAc-IdoA2S-GlcNS6S	**60**	GlcA-GlcNS-IdoA2S-GlcNS6S-GlcA-GlcNS
6	GlcA-GlcNAc-GlcA-GlcNAc	**34**	GlcA-GlcNS-IdoA-GlcNS6S	**61**	GlcA-GlcNAc-IdoA2S-GlcNS6S-IdoA2S-GlcNS
7	GlcA-GlcNAc-IdoA-GlcNAc	**35**	IdoA-GlcNS6S-GlcA-GlcNS	**62**	GlcA-GlcNS6S-GlcA-GlcNS6S-GlcA-GlcNS6S
8	GlcA-GlcNAc-IdoA2S-GlcNAc	**36**	IdoA2S-GlcNAc6S-GlcA-GlcNAc6S	**63**	GlcA-GlcNS6S-IdoA-GlcNS6S-GlcA-GlcNS6S
9	GlcA-GlcNAc-GlcA2S-GlcNAc	**37**	IdoA2S-GlcNS-GlcA-GlcNS	**64**	GlcA-GlcNS6S-GlcA-GlcNS6S-IdoA-GlcNS6S
10	GlcA-GlcNAc-IdoA-GlcNAc6S	**38**	GlcA-GlcNS6S-IdoA-GlcNS	**65**	GlcA-GlcNS6S-IdoA-GlcNS6S-IdoA-GlcNS6S
11	IdoA-GlcNAc6S-GlcA-GlcNAc	**39**	IdoA-GlcNS-IdoA-GlcNS6S	**66**	GlcA-GlcNS-IdoA2S-GlcNS6S-IdoA2S-GlcNS
12	IdoA2S-GlcNAc-GlcA-GlcNAc	**40**	GlcA-GlcNAc6S-GlcA2S-GlcNAc6S	**67**	GlcA-GlcNAc6S-IdoA2S-GlcNS6S-IdoA2S-GlcNS
13	IdoA-GlcNAc-IdoA-GlcNAc6S	**41**	IdoA-GlcNS6S-GlcA-GlcNS6S	**68**	GlcA-GlcNS6S-IdoA2S-GlcNS6S-GlcA-GlcNS6S
14	IdoA-GlcNAc6S-IdoA-GlcNAc	**42**	GlcA-GlcNS6S-IdoA-GlcNS6S	**69**	GlcA-GlcNS6S-IdoA2S-GlcNS6S-IdoA-GlcNS6S
15	GlcA-GalNAc-GlcA-GalNAc4S	**43**	GlcA-GlcNS6S-GlcA-GlcNS6S	**70**	GlcA-GlcNS6S-GlcA-GlcNS6S-IdoA2S-GlcNS6S
16	IdoA-GlcNS-IdoA-GlcNAc	**44**	IdoA-GlcNS6S-IdoA-GlcNS6S	**71**	GlcA-GlcNS6S-IdoA-GlcNS6S-IdoA2S-GlcNS6S
17	IdoA-GlcNAc-IdoA-GlcNS	**45**	GlcA-GlcNS-GlcA2S-GlcNS6S	**72**	GlcA-GlcNS6S-IdoA2S-GlcNS6S-IdoA2S-GlcNS
18	IdoA-GlcNAc6S-IdoA-GlcNAc6S	**46**	GlcA-GlcNS-IdoA2S-GlcNS6S	**73**	GlcA-GlcNS6S-IdoA2S-GlcNS3S6S-GlcA-GlcNS6S
19	IdoA-GlcNAc6S-GlcA-GlcNAc6S	**47**	IdoA2S-GlcNS6S-GlcA-GlcNS	**74**	GlcA-GlcNS6S-IdoA2S-GlcNS3S6S-IdoA-GlcNS6S
20	GlcA-GlcNAc6S-IdoA-GlcNAc6S	**48**	IdoA2S-GlcNAc6S-IdoA2S-GlcNAc6S	**75**	GlcA-GlcNS6S-GlcA-GlcNS3S6S-IdoA2S-GlcNS6S
21	GlcA-GlcNAc6S-GlcA-GlcNAc6S	**49**	IdoA-GlcNS-IdoA2S-GlcNS6S	**76**	GlcA-GlcNS6S-IdoA-GlcNS3S6S-IdoA2S-GlcNS6S
22	GlcA-GlcNAc-GlcA2S-GlcNAc6S	**50**	IdoA2S-GlcNS6S-IdoA-GlcNAc6S	**77**	GlcA-GlcNS6S-IdoA2S-GlcNS6S-IdoA2S-GlcNS6S
23	GlcA-GlcNAc-IdoA-GlcNS6S	**51**	GlcA-GlcNS6S-IdoA2S-GlcNS6S	**78**	GlcA-GlcNS6S-IdoA2S-GlcNS3S6S-IdoA2S-GlcNS6S
24	GlcA-GlcNAc-IdoA2S-GlcNAc6S	**52**	IdoA2S-GlcNS6S-GlcA-GlcNS6S	**79**	IdoA2S-GlcNS6S-IdoA2S-GlcNS6S-IdoA2S-GlcNS6S
25	IdoA2S-GlcNAc6S-GlcA-GlcNAc	**53**	IdoA-GlcNS6S-IdoA2S-GlcNS6S	**80**	GlcA-GlcNS6S-IdoA-GlcNS-IdoA2S-GlcNS6S-IdoA-GlcNAc6S
26	GlcA-GlcNS6S-GlcA-GlcNAc	**54**	GlcA-GlcNS3S-IdoA2S-GlcNS6S	**81**	IdoA2S-GlcNS6S-IdoA2S-GlcNS6S-IdoA2S-GlcNS6S-IdoA2S-GlcNS6S
27	GlcA-GlcNS6S-GlcA-GlcNAc	**55**	IdoA2S-GlcNS6S-IdoA2S-GlcNS	**82**	Heparin functionalized with primary amine (MW 27KDa)
28	IdoA-GlcNS-IdoA-GlcNS				

Figure 1. Binding of synthetic heparan sulfate oligosaccharides to SARS-CoV-2-spike and RBD. (A) Binding of SARS-CoV-2-spike (10 µg/mL) to the HS microarray. The strongest binding structures are shown as inserts. (B) Binding of SARS-CoV2-RBD (30 ug/mL) on the HS microarray. (C) Compounds numbering and structures of a selected part of heparan sulfate library.

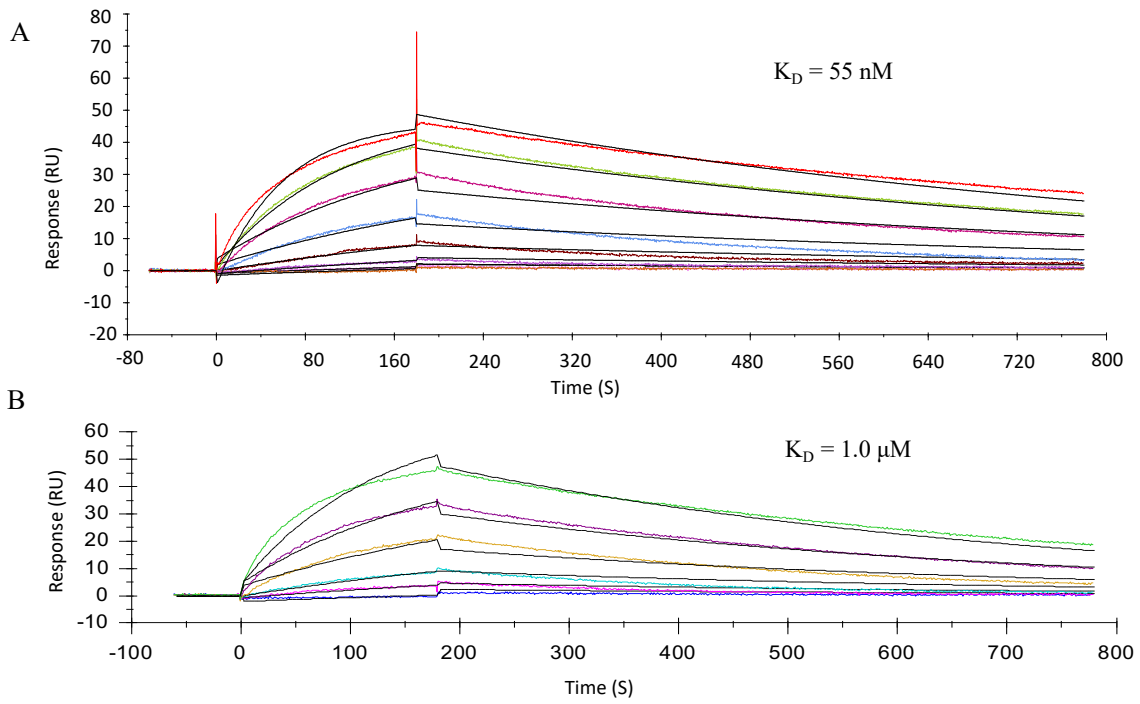

Figure 2. Sensorgrams representing the concentration-dependent kinetic analysis of the binding of (A) SARS-CoV-2 spike and (B) RBD with immobilized biotin-HG-Hep on a CM5 chip immobilized with SA. Concentrations of spike and RBD (from top to bottom) are 2-fold dilution from 446 to 6.97 nM and 11 to 0.34 μM, respectively. The black lines are fitted curves using a Langmuir 1:1 binding model.

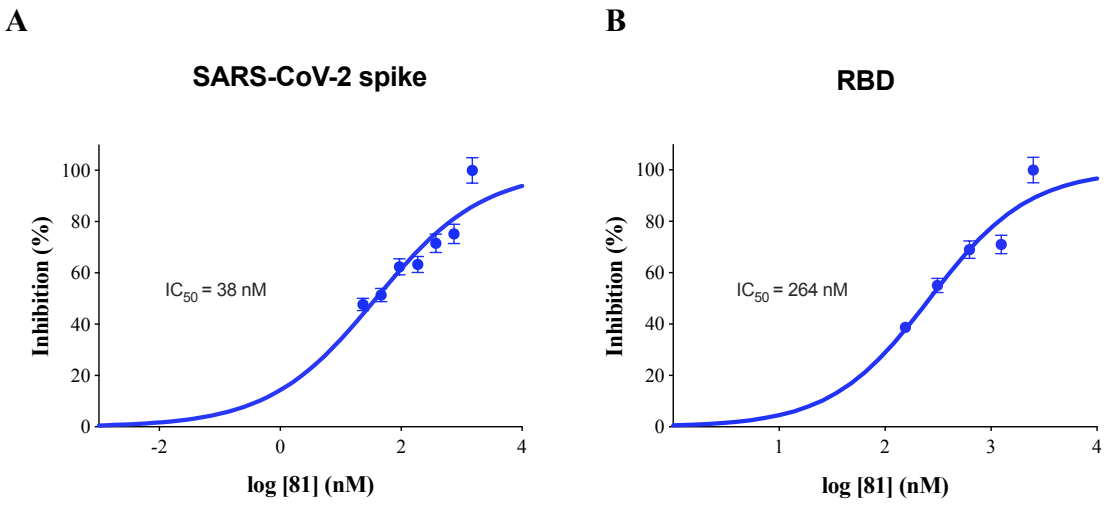

Figure 3. Inhibition analysis of **81** on the interaction of (A) SARS-CoV-2 spike and (B) RBD with HG-Hep. Concentration of spike and RBD were 150 nM and 2.4 μM, respectively. The dose response curves for IC_{50} calculation were derived from the inhibition data using surface competition SPR.